Transdisciplinary Engineering: Crossing Boundaries
M. Borsato et al. (Eds.)

doi:10.3233/978-1-61499-703-0-483

Aerodynamic Features Optimization of Front Wheels Surroundings for Energy Efficient Car

Mateusz WĄSIK[a,1] and Wojciech SKARKA[b]
[a] *Silesian University of Technology, Machine Technology Department*
[b] *Silesian University of Technology, Institute of Fundamentals of Machinery Design*

Abstract. Constant development of the vehicles energy efficiency, the fuel prices and the requirements for greenhouse gas emissions force designers to find new solutions to achieve the goals by minimising the movement resistances. As it was calculated basing on the research carried out at the Silesian University of Technology, the Institute of Fundamentals of Machinery Design on energy efficient cars designed for the Shell Eco-marathon race, the main component of the total resistance of a moving car is the aerodynamic drag which is equal, in such a type of car, to about 70% of the total movement resistance. The idea of the research is to optimize the shape of aerodynamic features of the front wheels surroundings. By the front wheel surroundings aerodynamic features, the front wheel arch and front bumper shapes are understood. The air drag depends on the elements of the drag coefficient c_x which is strongly connected with its shape and its area. Front wheel in motion rotates and generates air turbulences which have negative influence on the car aerodynamics. In majority of the cars the front wheels are swivel, which makes it difficult or impossible to close the front wheel arch. For reduction of the air drag generated by the open wheel arch, three types of solutions are designed and optimized. The first solution is the main shape of the analysed car parts which are shaped so that they generate minimal aerodynamic drag and lead the air stream to bypass the wheel niche. The second analysed solution is passive system consisting of respectively shaped holes in the front bumper. The holes lead the air stream into the wheel niche, equalize pressure in the wheel niche and reduce the air turbulences generated by the rotating wheel. The last solution is a set of overlays which lead the air stream in such a way to avoid its disruption to the wheel arch niche and achieve the best air stream distribution around the vehicle.

Keywords. Finite element method, Energy efficient car, Aerodynamics, CFD

Introduction

Constant development of the vehicles energy efficiency, the fuel prices and the requirements for greenhouse gas emissions force designers to find new solutions to achieve the goals by minimising the movement resistances [1,2]. As it was calculated basing on the research carried out at the Silesian University of Technology, the

[1] Corresponding Author, E-Mail: mateusz.wasik@polsl.pl

Institute of Fundamentals of Machinery Design on energy efficient cars designed for the Shell Eco-marathon race, the main component of the total resistance of a moving car is the aerodynamic drag which is equal, in such a type of car, to about 70% of the total movement resistance [3,4,5]. The idea of the optimization is to optimize the shape of the front wheel surroundings aerodynamic features. By the front wheel surroundings aerodynamic features, the front wheel arch and front bumper shapes are understood. The air drag depends on the elements of the drag coefficient c_x which is strongly connected with its shape and its area. Front wheel in motion rotates and generates air turbulences which have negative influence on the car aerodynamics. In most of the cars the front wheels are swivel which makes it difficult or impossible to close the front wheel arch.

Numerical computational aerodynamic studies represent a significant part in the design and optimization of car bodies. In comparison with tunnel based research, carrying out research using numerical methods [6,7] is relatively faster and less expensive. Based on numerical methods of calculation it is possible to simulate any ambient conditions, referred to as boundary conditions and visualize the distribution of parameter values as desired, for example the pressure distribution on the surface of the vehicle or the air speed distribution in the plane coinciding with the plane of symmetry of the car. Depending on the developed model, numerical methods [6,7] could provide high accuracy data. Their results can be compared with ongoing tunnel research on the physical model. This type of research—using virtual models created in a CAD environment eliminates necessity to manufacture physical model of the object of every developed version of optimized object, which significantly increases the costs of development process. Such approach makes it possible to determine the right direction of its development and to optimize its shape for the lowest aerodynamic drag in the early stages of the car body surface design process. Optimisation of vehicle aerodynamics considering its influence on total vehicles movement resistance is extremely important. It allows a significant reduction in the size of the required power units, which is associated with reduction of vehicle total weight and the energy absorbed by the power unit. Due to the continually rising fuel prices as well as environmental considerations in the current trend of the development of the automotive industry, vehicle weight reduction and energy consumption are very important issues.

1. Theoretical description of the studied phenomena

In fluid mechanics, there are different flow distributions due to different criteria. From the aerodynamics point of view, the division of flow due to the motion of fluid particles is important [2,3]. Consistent with this criterion the flow may be laminar or turbulent. Laminar flow [7] is a stratified flow, where the fluid flow creates a parallel, smooth layer. Depending on the shape of the walls of the object on which the fluid passes, the flow lines are straight or gently curved. The flow of this type is for small and medium speed for contractual Reynolds numbers less than *2300*. Turbulent flow [7] is characterized by the presence of time-varying flow disturbances, so-called turbulences, manifesting with blenders fluid particles. The characteristics of the flow are variable in time and space. Turbulent flow occurs at high flow velocities Reynolds numbers above *2300*.

Aerodynamic forces acting on the car in motion in air [8,9]. have several components. The components of the aerodynamic force relevant to the issues to be analysed are components acting along the longitudinal axis of the vehicle (so-called drag force) P_x (1) and the lift P_z (2).

$$F_x = \frac{1}{2} * \rho * S * v^2 * c_x \quad (1)$$

$$F_z = \frac{1}{2} * \rho * S * v^2 * c_z \quad (2)$$

where:

ρ is the air density, S the surface area of the object, v the speed, c_x coefficient of drag forces.

Other forces and moments acting on the car in motion are the lateral force *Fy*, the pitching moment *My,* heeling moment *Mx,* deflection moment *Mz*.

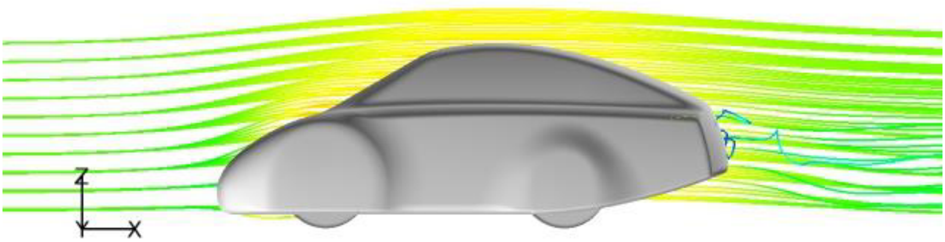

Figure 1. Flow directions in CFD aerodynamics.

Aerodynamic resistance [8÷11] is a movement counter force. Natural coordinate system of the tested issue is the coordinate system of a vehicle. However, it is preferable to adopt analysis system associated with the axes of the vehicle, since the vehicle is stationary and air is moving. A very important factor for consideration for car aerodynamic drag is a dimensionless drag coefficient c_x [8÷11]. It is associated with the shape of the body. The greater the drag coefficient, the greater the aerodynamic drag of the vehicle. Coefficient c_x is determined by measuring analytically drag forces. Boundary layer [8÷11] is a layer of medium flowing in a short distance from the surface of the test object. In the boundary layer, there are significant changes in speed. On the surface of the object the speed of of medium flowing over the test object is equal to zero, and increases to the set speed with the distance from the surface. The phenomenon of the boundary layer is related to the fluid viscosity. It is very difficult to determine unambiguously the thickness of the boundary layer. It is assumed that the value of the boundary is the place where the speed is 1% in comparison with the set speed.

2. Methodology

2.1. Aerodynamics CFD

The aerodynamic simulations were preformed in a virtual wind tunnel with a length of 15.5 m, height of 2.5 m and width of 1.2 m Due to the vehicle symmetry the analyses were conducted for its half to reduce the computing time. The selection of the tunnel size [10,11] parameters has been carried out experimentally. The length and height of the tunnel were selected on the basis of air velocity distribution on the vehicles symmetry plane. The tunnel width was selected so that the side turbulence lines do not exceed the tunnel borders. The object of interests was the vehicle front wheel surrounding. To increase the simulation accuracy, the ground movement and rotation of the front wheels were applied. The vehicles drag surface was covered with 7-layer boundary layer. Simulations were performed for a medium flowing in the form of air, having a temperature of 25°C, pressure of 1013,25 hPa (1 atm) and an initial speed of 10 m/s. As a model for the simulation of turbulence Spalart-Almaras model with turbulence coefficient equal to 5% was used. As a baseline for the analysis of air flow in the wind tunnel default software parameters were adopted. Any deviation from the baseline parameters used in the analysis are the parameters that give adequate accuracy at the same time the demand for computing power. Simulation conditions were chosen according to the conditions during the Shell Eco-marathon race in Rotterdam and in accordance with generally accepted principles of research in the tunnel of the Institute of Aviation in Warsaw [10,12]. In this study, it was achieved by the distribution of the drag forces and pressure distribution on the surface of the vehicle. On the basis of the obtained values of the aerodynamic drag force on the surface of the vehicle aerodynamic coefficient c_x was analytically calculated (1). The obtained results were validated analysing result change due to the mesh size change. The model was regarded as correct when the further decrease of the FEM [13,14] mesh size does not significantly change the obtained results.

2.2. Optimization

Optimization process [15÷18] consists of a couple of sub processes (Figure 2). Based on the simplified CAD model, the vehicle is aerodynamically analysed according to the methodology described in the *Methodology* chapter.

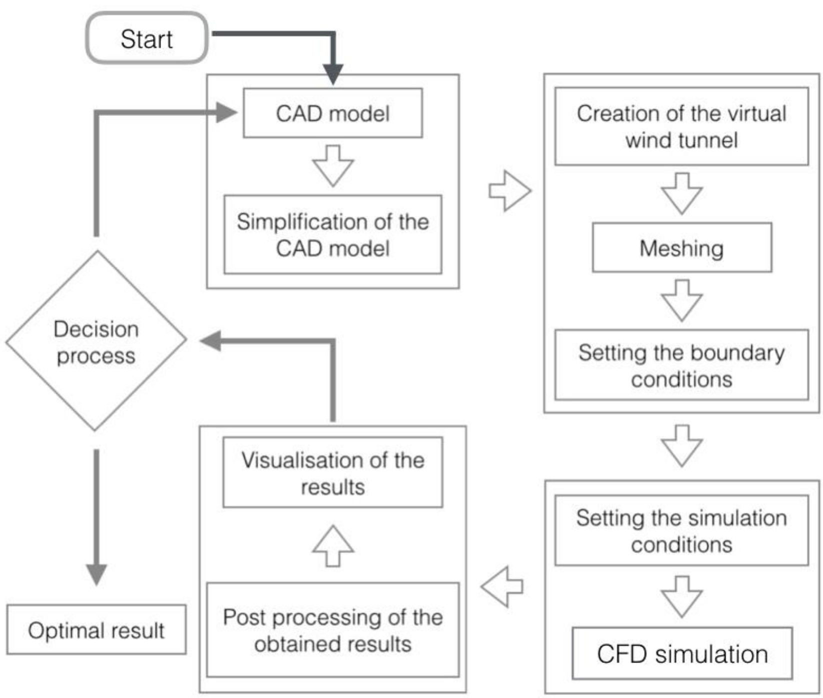

Figure 2. Optimization methodology diagram [19,20].

The optimization was carried out iteratively. After each iteration the set of obtained results was analysed — the drag coefficient, the drag force of the whole vehicle and the flow streamline distribution in the front wheel surrounding. Then it was decided if the solution can be considered as an optimal one and the optimization can be stopped, or should be changed and the optimization should be continued.

Firstly, the problem ratio was indicated. The streamlines for the basic version of the front wheel surrounding are the indicators of the areas that are disturbing the air streamlines in that way that the drag force of vehicle increases. In the second phase of optimization the shape of the wheels surrounding parts were optimized, i.e.—front bumper and front wheel arch. The criteria of reduction are their drag coefficient and achievement of the optimal streamline distribution to avoid its falling into the wheel arch hole (Figure 3). The next step of optimization was to design and optimize a set of holes in the front bumper that will lead the part of the air stream from the place with the highest pressure (the tip of the bumper) to the wheel arch hole to blow out the turbulent air from its inside. The last part of optimization was to design and optimize additional deflectors for the front wheels surrounding that lead the blow out stream from the wheel arch hole. The optimization has been stopped when, the further shape changes were not giving satisfactory improvement and the size limits were achieved.

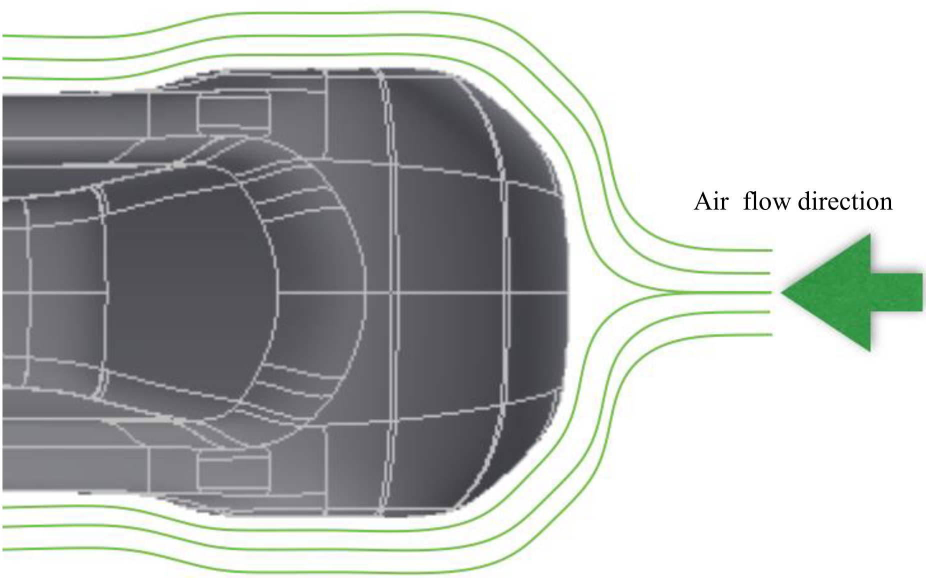

Figure 3. Visualisation of the protection shield idea.

The geometry has been parametrized. In optimization process the set of the geometric parameters has been changing selectively. Parametrization includes the design variables relation and assumption that the cross sections of optimized parts (inlet channels) are constant to avoid air flow turbulences. In the optimization process possible wide parameter area was searched. The design parameter sets are different for each optimized part. For the inlet channels parametrization the authors decided tofollow such design parameters as size and shape of the channels inlet cross section. For the front bumper parametrization the authors decided to follow design the following parameters: radii of curvatures of the bumpers cross section in two perpendicular surfaces with assumption of constant width of the bumper. For the wheel arch deflector parametrization the authors followed such design parameters as width, height, length of the deflector and the curvature radius of the deflector face.

3. Results

The base for identification of the critical regions was the visualisation of the pressure distribution on the vehicle surface. As it can be recognized (Figure 4) the highest pressure appears on the front tip of the vehicle. From this area all of the air streamlines begin to encircle the vehicle. Other region that can be mentioned according to the optimization of the front wheel surroundings is the back wall of the front wheel arch hole. It is a region of high air pressure caused by combination of the wheel rotation and irruption of the air stream encircling the bottom part of the vehicle.

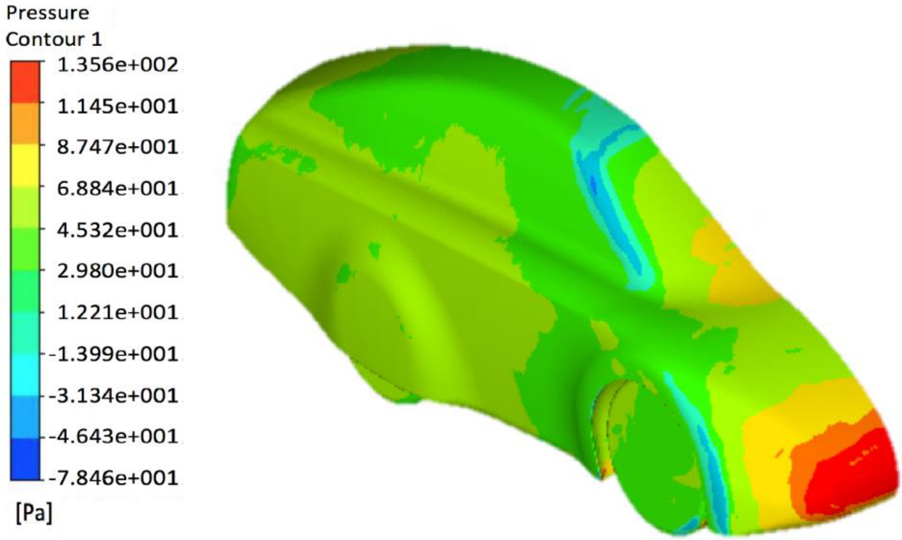

Figure 4. Visualisation of the pressure distribution on the vehicles surface before optimization.

3.1. Optimization of the front bumper shape

After the first optimization stage—optimization of the front bumper shape, the vehicles aerodynamic characteristic has been changed. In the table (Table 1) the optimization results are included. The first compared bumper version (Bumper v1*) is the input, non optimized version of the vehicles part. As it can be observed the total vehicles drag coefficient c_x and its aerodynamic drag force decrease for the next optimized versions. Comparing the results for input bumper version with the best achieved solution, the drag coefficient c_x and drag force were reduced by 15%. The drag area has not changed significantly.

Table 1. Comparison of the results for optimized bumper shape.

	Vehicles drag coefficient c_x	**Vehicles drag force [N]**	**Drag area [m²]**
Bumper v1*	0,3498	21,66	1,059
Bumper v2	0,3198	19,80	1,060
Bumper v3	0,3195	19,78	1,065
Bumper v4	0,2997	18,57	1,060

3.2. Optimization of the front bumpers inlet channel.

After the second optimization stage—optimization of the front bumper inlet tunnels (Figure 5) the vehicles aerodynamic characteristic has been also changed. According to the figure (Figure 5) the air from the region of highest pressure gets into the inlet tunnel reducing the air pressure on the bumpers tip. The outlet of the tunnel is located inside the wheel arch gap. The tunnel has constant cross section over the entire length to minimize the flow turbulences. The air stream incoming through the tunnel blows off the turbulent air stream generated as the consequence of the wheel rotation. In the table (Table 2) the optimization results are included. The first compared bumper version (w/o tunnels*) is the input part from the first step of optimization without inlet channel. The decrease can be observed of the vehicles coefficient c_x and its aerodynamic drag force. The exception is the *Tunnel v1* which significantly increases the drag area what affects the higher vehicle drag coefficient. For every version of the inlet tunnels the increase of the drag area can be observed which is caused by the appearance of additional drag surfaces inside the front bumper.

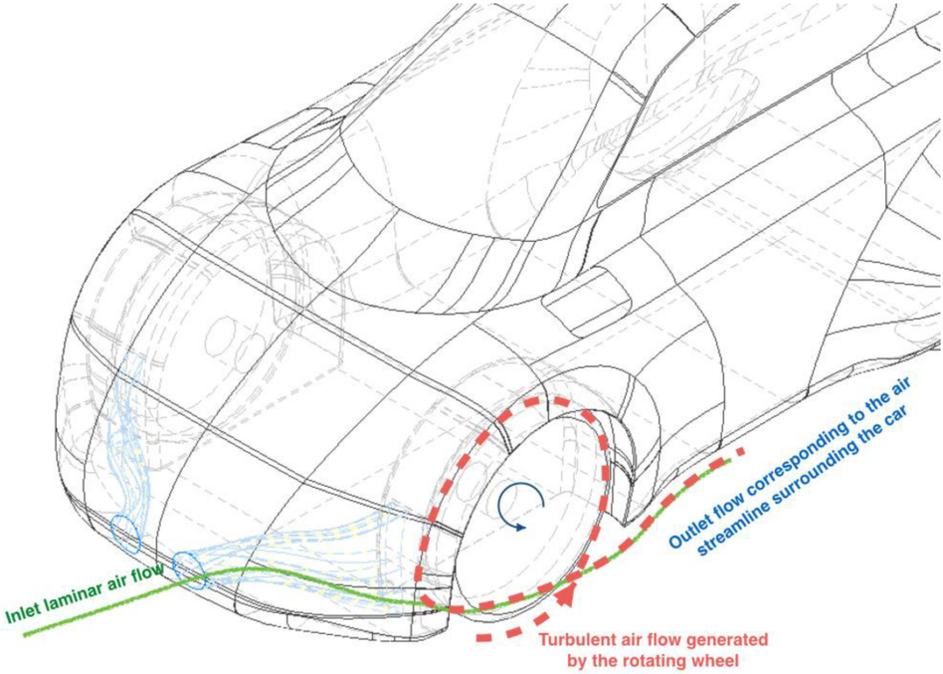

Figure 5. Front bumper air flow tunnels principle of operation.

Comparing the results for input bumper version with the best achieved solution, the drag coefficient c_x and drag force were reduced by 8%.

Table 2. Comparison of the results for optimized bumper inlet tunnels.

	Vehicles drag coefficient c_x	**Vehicles drag force [N]**	**Drag area [m^2]**
w/o tunnels*	0,2997	18,57	1,060
Tunnel v1	0,3101	20,12	1,090
Tunnel v2	0,2850	18,51	1,063
Tunnel v3	0,2769	17,97	1,062

3.3. Optimization of the wheel arch surrounding.

After the last optimization stage—optimization of the wheel arch surrounding (Figure 6) the vehicles aerodynamic characteristic has also been changed. In the table (Table 3) the optimization results are included. The first compared bumper version (w/o deflector*) is the last geometry of the second stage optimization.

The deflector (Figure 6) is mounted inside the wheel arch gap to lead the air stream generated by the wheel rotation in the way that it changes its back edge and minimizes the air pressure inside. The air stream irruption into the wheel arch gap was significantly reduced with the front bumper shape so the deflector helps to reduce the influence of the turbulent flow generated by the rotating wheel.

The slight decrease can be observed of the vehicles drag coefficient c_x and its aerodynamic drag force. The exceptions are the *Deflector v1* which bring no significant changes or and *Deflector v2* which has negative influence on the vehicles aerodynamic drag. For every version of this solution only a little increase of the drag area can be observed which is caused by the low drag area of the deflector. Comparing the results for input bumper version with the best achieved solution, the drag coefficient c_x and drag force were reduced by 2%.

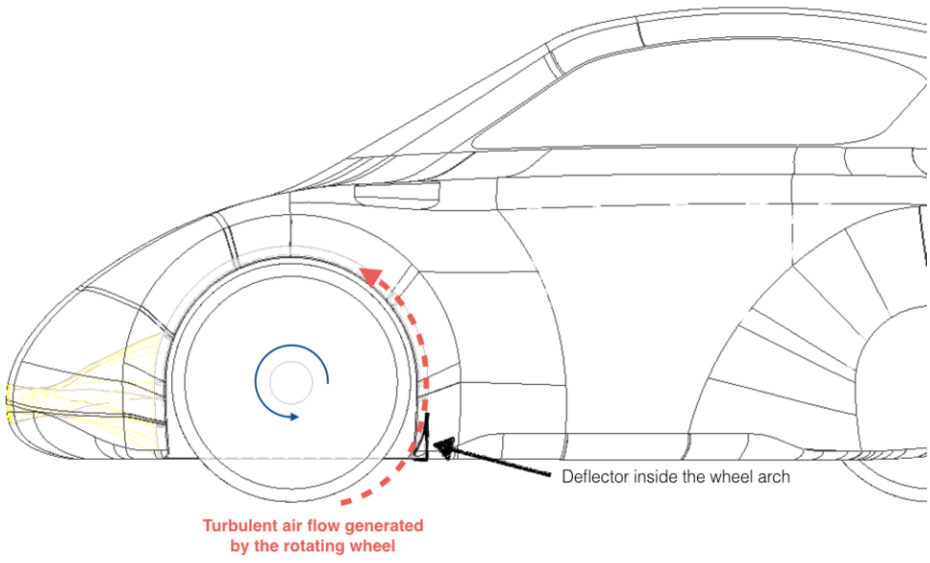

Figure 6. Wheel arch deflector principle of operation.

Table 3. Comparison of the results for optimized wheel arch surrounding.

	Vehicles drag coefficient c_x	Vehicles drag force [N]	Drag area [m^2]
w/o deflector*	0,2769	17,97	1,062
Deflector v1	0,2771	18,04	1,063
Deflector v2	0,2830	18,42	1,062
Deflector v3	0,2714	17,67	1,062

4. Conclusions

The research contains the optimization of the front wheels surrounding of the energy efficient car. By changing the front bumper shape, adding inlet tunnels and deflector the irruption of the air flow streamline into the wheel arch gap was reduced which consequently leads to reduction of the vehicles air drag. In the total optimization process 23% reduction of the vehicles drag coefficient c_x was achieved. The design changes affect also the air pressure distribution on the vehicles surface (Figure 7). The regions of high pressure were significantly reduced and the high air pressure on the tip of the front bumper was used to reduce the air pressure inside the wheel arch gap. As it can be noticed the optimization was carried out for the case when the car moves straight. The impact of the stream at an angle – change of the direction of the car cases were not analysed. Due to the different and non-symmetric wheels arrangement (when the car turns the left wheel position in relation to the wheel arch gap is different than the right wheels) such solution may bring different, even worse results than the non-optimized one. Improving the optimized vehicle with movable deflectors—flap regulation in the bumper inlet tunnels and movable deflector at the ends of the front bumper can adjust such solution for different turn angles.

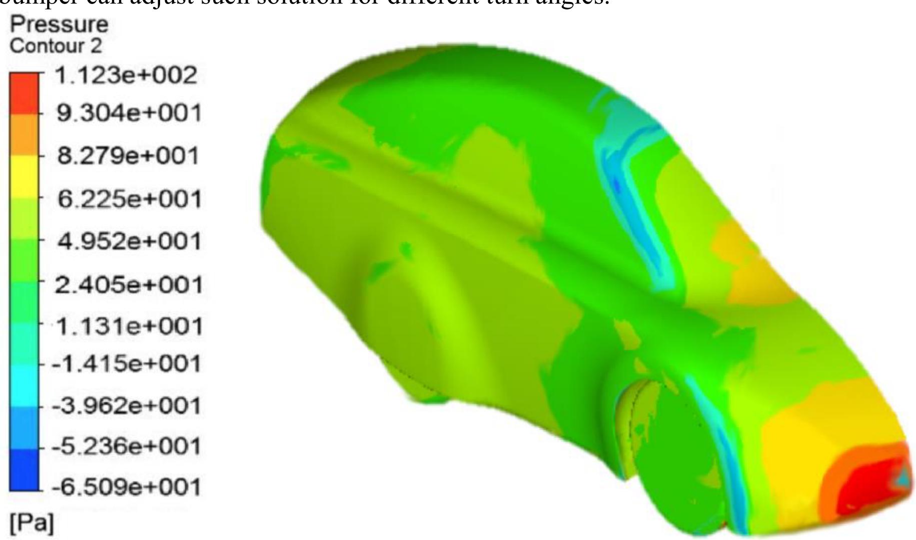

Figure 7. Visualisation of the pressure distribution on the vehicles surface after optimization.

Considering the fact, that for such a vehicle the 70% of the movement resistance is the aerodynamic drag, such solution which reduces the air drag by 23% can meaningfully improve vehicles energy efficiency. It is particularly essential in comparison with ending resources of fossil fuels and pollution and thermal gases emission reduction. Applied changes in analysed vehicle give significant air drag reduction. Optimized issues were observed in CFD simulations. The vehicle was manufactured as a prototype and takes part in Shell Eco-marathon competition. Conducted optimization is an answer for the need to reduce the movement resistances of existing vehicle. Further air drag reduction will require new body design.

References

[1] K. Sternal, A. Cholewa, W. Skarka, M. Targosz, Electric Vehicle for the Students' Shell Eco-Marathon Competition. Design of the Car and Telemetry System, In: J. Mikulski (ed.) *Telematics in the Transport Environment, 12th International Conference on Transport Systems Telematics, TST 2012*, Katowice-Ustroń, Poland, October 10–13, 2012, Communications in Computer and Information Science, Springer, Berlin Heidelberg, 2012, pp. 26-33.

[2] W. Skarka, Reducing the Energy Consumption of Electric Vehicles, In: R. Curran et al. (eds.), *Transdisciplinary Lifecycle Analysis of Systems. Proceedings of the 22nd ISPE Inc. International Conference on Concurrent Engineering*, Delft, The Netherlands, July 20-23, IOS Press, Amsterdam, 2015, pp. 500-509.

[3] W. Skarka, Application of numerical inverse model to determine the characteristic of electric race car, In: I. Horvath et al. (eds.), *Tools and methods of competitive engineering*. TMCE 2014 Symposium, Budapest, Hungary, May19-23, 2014, pp. 263-274.

[4] M. Targosz, M. Szumowski, W. Skarka, P. Przystałka, Velocity Planning of an Electric Vehicle Using an Evolutionary Algorithm, In: J. Mikulski (ed.) *Activities of Transport Telematics, 13th International Conference on Transport Systems Telematics, TST 2013*, Katowice-Ustron, Poland, October 23-26, 2013, Communications in Computer and Information Science, Springer Berlin Heidelberg (2013), pp. 171-177.

[5] M. Targosz, W. Skarka, P. Przystałka, Simulation and optimization of prototype electric vehicle Methodology, In: D. Marjanovic et al. (eds.) *Proceedings of the 13th International Design Conference*, Dubrovnik, Croatia, May 19-22, 2014, pp. 1349-1360.

[6] J.D.Anderson, JR., *Computational Fluid Dynamics: The basics with applications*, McGraw-Hill, Inc., New York, 1995.

[7] F.M. White, *Fluid Mechanics,*4th ed, McGraw-Hill College, 1998.

[8] H. Smith, *Illustrated Guide to Aerodynamics*. TAB Books, 1992.

[9] W.H. Hucho, *Aerodynamic of Road Vehicles,* Butterworths Co., Ltd., 1997.

[10] A. Pope, *Wind Tunnel Testing,* 2nd ed, John Wiley & Sons, New York, 1974.

[11] J.H. Ferziger, M. Peric, *Computational Methods for Fluid Dynamics*, Springer, New York, 2002.

[12] Institute of Aviation in Warsaw, Accessed: 18.04.2016 [online] Available: http://ilot.edu.pl/en/.

[13] T.R. Chandrupatla, A.D. Belegundu, *Introduction to finite element method in engineering*, Prentice-Hall, London, 1991.

[14] R.D. Cook, *Concept and applications of finite element analysis*, Wiley, New York, 1981.

[15] W.H. Press, S.A. Teukolsky, W.T. Vetterling, B.P. Flannery, *Numerical recipes in C. The art of scientific computing*, 2nd ed, Cambridge University Press, Cambridge, 1992.

[16] D.C. Liu, J. Nocedal, On the limited memory BFGS method for large-scale optimization. *Mathematical Programming*, 45, 1989, pp. 503-528.

[17] T. Weise, *Global Optimization Algorithms – Theory and Application*, 2nd ed, IT Weise, 2009.

[18] A. Neumaier, Complete search in continuous global optimization and constraint satisfaction, *Acta Numerica*, 13, 2004, pp. 271–369.

[19] M. Wąsik, Influence of the windscreens inclination angle on the aerodynamic drag coefficient of the cars participating in the race Shell Eco-marathon based on numerical simulations, In: J. Maczak (ed.) *XIV International Technical Systems Degradation Conference*, Liptovsky Mikulas, 8-11 April 2015, Faculty of Automotive and Construction Machinery Engineering, Warsaw University of Technology. Polskie Naukowo-Techniczne Towarzystwo Eksploatacyjne, Warszawa, 2015, pp. 158-160.

[20] M. Wąsik, Methodology of aerodynamic analysis of the cars participating in the race shell Eco-marathon based the HyperWorks software, In: J. Maczak (ed.) *XIII International Technical Systems Degradation Conference*, Liptovsky Mikulas, 23-26 April 2014. Polskie Naukowo-Techniczne Towarzystwo Eksploatacyjne, Warszawa, 2014, pp. 119-120.